



PERGAMON

Available online at www.sciencedirect.com

SCIENCE @ DIRECT®

Planetary and Space Science 51 (2003) 365–373

**Planetary
and
Space Science**www.elsevier.com/locate/pss

Kinetics of suprathreshold hydrogen atom reactions with saturated hydrides in planetary and satellite atmospheres

Richard J. Morton, Ralf I. Kaiser*

Department of Chemistry, University of York, YO10 5DD, UK

Received 3 April 2002; received in revised form 12 February 2003; accepted 12 March 2003

Abstract

The kinetics of saturated hydrides methane (CH₄), silane (SiH₄), germane (GeH₄), ammonia (NH₃), phosphine (PH₃), arsane (AsH₃), water (H₂O), and hydrogen sulfide (H₂S) in the low-temperature atmospheres of Jupiter, Saturn, Uranus, Neptune, Pluto, Titan, and Triton reacting with suprathreshold hydrogen atoms were investigated computationally to extract suprathreshold rate constants $k(E)$ via an inverse Laplace transformation from experimentally available thermal rate constants $k(T)$. Our data reveal that all suprathreshold rate constants range up to 10^{-10} cm³ s⁻¹, whereas the thermal counterparts are as low as 8×10^{-73} cm³ s⁻¹. These data demonstrate explicitly a significantly enhanced reactivity of photolytically generated suprathreshold hydrogen atoms in the low-temperature planetary and satellite atmospheres and suggest that this hitherto unaccounted reaction class should be included by the planetary modeling community into future photochemical networks of atmospheres of outer solar system planets and their moons.

© 2003 Elsevier Science Ltd. All rights reserved.

Keywords: Planetary atmospheres; Non-equilibrium chemistry; Cometary chemistry; Hydrogen atoms; Hydrides

1. Introduction

Simple saturated hydrides present important chemical constituents in the atmospheres of outer solar system planets, their moons (Yung and DeMore, 1999), and comets (Rodgers and Charnley, 1998). The Voyager missions, star occultations, and terrestrial-based telescopes identified methane (CH₄) in the atmospheres of the four giant planets Jupiter (Sada et al., 1998; Maillard et al., 1995; Encrenaz et al., 1995; Strong et al., 1993; Ortiz et al., 1992; Molina and Moreno, 1992; Satoh and Kawabata 1992; Moreno et al., 1991; Molina and Moreno, 1992), Saturn (Ortiz et al., 1993), Uranus (Baines et al., 1995; Smith et al., 1990), and Neptune (Baines et al., 1995; Baines and Hammel, 1994; Romani et al., 1993; Debergh et al., 1990; Romani and Atreya, 1989), as well as Pluto (Stansberry et al., 1996), Titan (Tokano et al., 2001; Kim et al., 2000; Wilson and Atreya, 2000; Lunine et al., 1999; McKay et al., 1997; Samuelson and Mayo, 1997; Samuelson et al., 1997; Ricard et al., 1995; Karkoschka, 1994; Borysow and Tang, 1993;

Thompson et al., 1992; Thompson et al., 1991; Karkoschka, 1998), and Triton (Stansberry et al., 1996; Herbert and Sandel, 1991; Strobel et al., 1990) (Table 1). Germane (GeH₄), arsane (AsH₃), and ammonia (NH₃) have also been found on Jupiter (Molina and Moreno, 1992; Nava et al., 1993; de Pater et al., 2001; Fouchet et al., 2000; Edgington et al., 1998, 1999; Folkner et al., 1998; Roos-Serote et al., 1998; Edgington et al., 1998; Lara et al., 1998; Davis et al., 1997; Griffith et al., 1992; Molina and Moreno, 1992; Ferris et al., 1992; Noll and Larson, 1991) and Saturn (Nava et al., 1993; Chen et al., 1991) with upper limits of NH₃ derived in Uranus's (Hofstadter and Muhleman, 1989) and Neptune's atmosphere (Yung and DeMore, 1999). Phosphine (PH₃) (Edgington et al., 1998; Lara et al., 1998; Davis et al., 1997; Griffith et al., 1992; Borunov et al., 1995; Orton et al., 2000; Weisstein and Serabyn, 1994; Noll and Larson, 1991; Encrenaz et al., 1996) and water (H₂O) (Roos-Serote et al., 1998; Bergin et al., 2000; Simon-Miller et al., 2000; Gibbard et al., 1995; Noll et al., 1995; Delgenio and McGrattan, 1990; Dowling and Ingersoll, 1989; Joiner et al., 1992; Degraauw et al., 1997) are present on all of the four giant planets as well. Hydrogen sulfide (H₂S) has only been detected on Jupiter (Yung and DeMore, 1999), but upper limits have been derived for Saturn, Uranus (de Pater

* Corresponding author. Present address: Department of Chemistry, University of Hawaii at Manoa, 2545 The Mall, Honolulu, HI 96822, USA.

E-mail address: kaiser@gold.chem.hawaii.edu (R.I. Kaiser).

Table 1

Average relative abundances of simple hydrides in the atmospheres of the outer solar system planets and their moons

	Jupiter	Saturn	Uranus	Neptune
CH ₄	3.0×10^{-3}	4.5×10^{-3}	2.3×10^{-2a}	2.0×10^{-2b}
GeH ₄	7.0×10^{-10}	4.0×10^{-10}	—	—
NH ₃	2.6×10^{-3}	2.0×10^{-4}	$< 1.0 \times 10^{-7}$	$< 6.0 \times 10^{-7c}$
PH ₃	7.0×10^{-7}	1.4×10^{-6}	5.0×10^7	3.0×10^{-5}
AsH ₃	2.2×10^{-10}	3.0×10^{-9}	—	—
H ₂ O	3.0×10^{-5d}	2.0×10^{-7e}	1.2×10^{-8f}	3.5×10^{-9g}
H ₂ S	6.1×10^{-6b}	$< 2.0 \times 10^{-7}$	$< 8.0 \times 10^{-7}$	$< 3.0 \times 10^{-6}$

“<” denotes upper limits. CH₄ has also been detected on Pluto (0.03), Titan (1.3×10^{-2}), and Triton (1.7×10^{-24}).

^a 2.3×10^{-2} in the troposphere, 2.0×10^{-5} in the stratosphere.

^b $< 8.6 \times 10^{-7}$ at 3.6 bar, 6.1×10^{-6} at 8.7 bar, 6.7×10^{-5} at $p > 16$ bar.

^cAt 130 K.

^d $3.0 \pm 2.0 \times 10^{-5}$ at 6 bar level, $4.0 \pm 1.0 \times 10^{-6}$ at 2–4 bar level.

^e 2.0×10^{-7} $p > 3$ bar in the troposphere.

^f 5.0 – 12.0×10^{-9} at $p < 0.003$ mbar in the stratosphere.

^g 1.5 – 3.5×10^{-9} at $p < 0.6$ mbar in the stratosphere.

et al., 1991), and Neptune (de Pater et al., 1991; Deboer and Steffes, 1994). So far, silane (SiH₄) has never been discovered in the atmosphere of any solar system planet. Only upper limits of 4×10^{-9} have been suggested for the atmosphere of Saturn (Yung and DeMore, 1999).

Although these saturated hydrides are only present in trace amounts, they are important for the chemical evolution of the atmospheres of planets and satellites. For instance, PH₃ and related phosphorus-bearing molecules are thought to be responsible for the reddish to brownish color of Jupiter (Griffith et al., 1992; Dowling and Ingersoll, 1989). CH₄ is discussed as the key precursor to form the organic haze layers on Titan and Triton. The reactions of hydrogen atoms with saturated hydrides are also of particular importance to the planetary modeling community (Deboer and Steffes, 1994; Samuelson and Mayo, 1997; Ollivier et al., 2000; Orton et al., 2000). The ultimate goal of those investigations is to compute the abundances of molecules in the atmospheres of the planets and their moons and to compare these with actual data derived from infrared, visual, or ultraviolet observations. These models require accurate input data on the reaction products and the rate constants. In general, kinetic models express the temperature-dependent rate constant $k(T)$ as a modified Arrhenius equation (Atkins, 1999):

$$k(T) = AT^{n-1/2}e^{-E_a/RT}, \quad (1)$$

where A is the pre-exponential factor, E_a the activation energy of the reaction, R the gas constant, T the temperature, where n is a real number. Since the temperatures of the planetary and satellite atmospheres are very low and range between 30 and 165 K (Table 2), rapid chemical reactions should have no or only a small activation energy E_a . In particular, the reactions of cyano (CN) and ethynyl (C₂H) radicals with unsaturated hydrocarbons were found to be very fast ($k(T) \approx 10^{-10} \text{ cm}^3 \text{ s}^{-1}$) over a temperature range of 13–293 K (Smith and Rowe, 2000), forming nitriles and complex unsaturated hydrocarbons, respectively, in Titan's

Table 2

The temperatures of the atmospheres of outer solar system planets and their moons

Planet/Moon	Temperature of the atmosphere (K)
Jupiter	165 ^a
Saturn	134 ^a
Uranus	76 ^a
Neptune	72 ^a
Pluto	30–44 ^b
Titan	94 ^a
Triton	38 ^c

^a $p = 1$ bar.

^b p (30 K) = 0.1 μ bar; p (44 K) = 500 μ bar.

^cTemperature at the surface, p (38 K) = 17.5 μ bar.

atmosphere (Balucani et al., 2000; Kaiser 2002). However, the reactions of hydrogen atoms with simple saturated hydrides of the generic form MH_{*n*}:



were postulated to be less important in these low-temperature environments, since they involve significant activation energies (cf. Table 3) (Deboer and Steffes, 1994; Samuelson and Mayo, 1997).

The activation energies cover a range from 5.97 kJ mol⁻¹ for H/AsH₃ to 85.22 kJ mol⁻¹ for the H/H₂O system. Since 11604.5 K is equivalent to 96.5 kJ mol⁻¹, the average temperature equivalent of these activation barriers is calculated to lie between 696 and 10,212 K on average. Those figures make it exceptionally clear that thermal reactions of the generic form of Eq. (2) are deemed to be less important in low-temperature planetary and satellite atmospheres. However, these models only consider reactions of thermal hydrogen atoms, but do not account for the reactivity of non-equilibrium (suprathermal) hydrogen atoms with saturated hydrides. Suprathermal species can be generated in

Table 3

Coefficients of the Arrhenius equation (1) of a bimolecular reaction (2) of simple hydrides with atomic hydrogen to form molecular hydrogen (Heyl, 1990; Mallard, 1994)

Hydride	A ($\text{cm}^3 \text{s}^{-1}$)	n	E_a (kJ mol^{-1})	E_a (eV)	E_a (\AA) ^a
CH ₄	1.00×10^{-10}	0.50	48.22	0.50	24,808
SiH ₄	2.30×10^{-11}	0.50	11.64	0.12	102,771
GeH ₄	1.94×10^{-10}	0.50	9.40	0.10	127,329
NH ₃	1.21×10^{-10}	0.50	57.50	0.60	20,804
PH ₃	4.50×10^{-11}	0.50	6.14	0.06	194,703
AsH ₃	2.57×10^{-10}	0.50	5.97	0.06	200,396
H ₂ O	1.50×10^{-10}	0.50	85.22	0.88	14,038
H ₂ S	1.50×10^{-11}	0.50	7.07	0.07	169,276

^aWavelength equivalent of activation energy.

Table 4

Solar spectral irradiance at 1 AU (1 astronomical unit (AU) = 1.496×10^{11} m)

Wavelength (\AA)	Fraction of energy flux	Photon flux ($\text{cm}^{-2} \text{s}^{-1}$)
1200	4.4×10^{-6}	2.0×10^{11}
2000	8.1×10^{-5}	1.1×10^{13}
2500	1.9×10^{-3}	2.5×10^{14}
3000	1.2×10^{-2}	2.3×10^{15}
3500	4.5×10^{-2}	9.1×10^{15}
4000	8.7×10^{-2}	2.0×10^{16}
5000	2.3×10^{-1}	6.4×10^{16}
8000	5.6×10^{-1}	2.2×10^{17}

Table 5

Bond energies of simple hydrides

Bond	Bond energy (kJ mol^{-1})	Bond energy (eV)	Bond energy (\AA) ^a
H–CH ₃	438.9	4.5	2725.6
H–SiH ₃	384.1	4.0	3114.4
H–GeH ₃	349.0	3.6	3427.7
H–NH ₂	452.7	4.7	2642.5
H–PH ₂	351.0	3.6	3408.1
H–AsH ₂	319.2	3.3	3747.7
H–OH	498.0	5.2	2402.1
H–SH	381.6	4.0	3134.8

^aWavelength equivalent of activation energy.

the atmospheres of the outer solar system planets and their moons by, for example, solar photons (Table 4) which can photodissociate hydrides to form atomic hydrogen and the corresponding radical (cf. Eq. (3)):



Considering reaction (3) as a typical example and accounting for the bond energy (Table 5) as well as momentum and energy conservation, solar photons of 2000 \AA can form hydrogen atoms with a kinetic energy of up to 137 kJ mol^{-1} (1.42 eV). This kinetic energy of a single hydrogen atom would correspond formally to a temperature

of 16,440 K. Therefore, photolytically generated hydrogen atoms are not in thermal equilibrium with the surrounding low-temperature atmospheres. If the kinetic energy of this suprathermal hydrogen atom is larger than the activation energy of a chemical reaction (2), this energy could be used to overcome this barrier. Therefore we expect that reactions of suprathermal hydrogen atoms are faster than their thermal counterparts. Unfortunately, experimental data on suprathermal rate constants are sparse, but nonetheless crucial to understand the chemical evolution of planetary atmospheres and their moons. This paper employs an inverse Laplace transformation (Arfken, 1985; Heyl and Roessler, 1990) to extract the suprathermal rate constants from experimentally available thermal data (cf. Section 2). The thermal rate constants are compared with their suprathermal counterparts, and the implications to planetary modeling and the evolution of the planetary atmospheres are discussed.

2. Methodology

In order to study the reactivity of suprathermal hydrogen atoms, it is essential to calculate the rate constant, $k(E)$, for each reaction at well-defined kinetic energy, E , of the suprathermal hydrogen atom. The rate constant $k(T)$ of a bimolecular reaction Eq. (2) at a temperature T is an integral folding the energy-dependent reaction cross section $\sigma(E)$ with the velocity distributions of the reactants. For a reaction between two reactants A and B holding the velocities $|\vec{v}_A|$ and $|\vec{v}_B|$, $k(T)$ is given by (Heyl and Roessler, 1990):

$$k(T) = \int_0^\infty \int_0^\infty f_A(|\vec{v}_A|) \cdot f_B(|\vec{v}_B|) \cdot \sigma(E) |\vec{v}_A - \vec{v}_B| d|\vec{v}_A| d|\vec{v}_B|. \quad (4)$$

Here, $f_A|\vec{v}_A|$ and $f_B|\vec{v}_B|$ are the velocity distributions of species A and B, respectively, $|\vec{v}_A - \vec{v}_B|$ corresponds to the relative velocity vector $|\vec{v}_r|$. Eq. (4) is versatile and allows us to calculate thermal as well as suprathermal reaction rate

constants. For suprathermal reactions, the energy-dependent cross section $\sigma(E)$ is often unknown. In those cases where neither theoretically calculated nor experimentally determined energy-dependent cross sections are available, a simple procedure can be used to derive $\sigma(E)$. This calculates the energy dependent cross section of suprathermal reactions from experimentally available thermal data. Considering a thermal reaction with a species A, the reactants are in thermal equilibrium and have a Maxwell–Boltzmann velocity distribution $f(|\vec{v}_A|)$:

$$f(|\vec{v}_A|) = 4\pi \cdot \left(\frac{m_A}{2\pi RT}\right)^{3/2} \cdot |\vec{v}_A|^2 \cdot e^{-m_A|\vec{v}_A|^2/2RT}, \quad (5)$$

where m_A the molar mass of reactant A, R the gas constant, T the temperature, and $|\vec{v}_A|$ the velocity of the reactant A. If the reactants are in thermal equilibrium and can be described as a Maxwell–Boltzmann distribution, $k(T)$ calculates via (4) and (5) to

$$k(T) = (\pi\mu)^{1/2} \left(\frac{2}{RT}\right)^{3/2} \int_0^\infty E\sigma(E) e^{-E_0/RT} dE. \quad (6)$$

Here, μ is the reduced mass,

$$\mu = \frac{m_A m_B}{m_A + m_B}, \quad (7)$$

m_A the mass of species A, and m_B the mass of species B. The relative energy E is given by

$$E = \frac{\mu}{2} |\vec{v}_A - \vec{v}_B|^2. \quad (8)$$

Eq. (6) is simply the Laplace transformation of the product $E \times \sigma(E)$ (Arfken, 1985) and can generally only be solved analytically. However, if the energy-dependent cross section $\sigma(E)$ follows Eq. (9), then an explicit solution is possible:

$$\sigma(E) = C \frac{(E - E_0)^n}{E}. \quad (9)$$

Here E_0 is the entrance barrier of a reaction, C is a constant, and n is an integer. Plugging Eqs. (8) and (9) into (6) and accounting for the integration limits gives:

$$k(T) = C2^{3/2}(\pi\mu)^{-1/2}(RT)^{n-1/2}\Gamma(n+1)e^{-E_0/RT} \quad (10)$$

with the Gamma function $\Gamma(n+1)$ (Lide, 1999). All non-temperature-dependent pre-exponential factors can be combined into a single constant A :

$$A = C2^{3/2}(\pi\mu)^{-1/2}(R)^{n-1/2}\Gamma(n+1). \quad (11)$$

Substituting Eq. (11) into Eq. (10) gives

$$k(T) = AT^{n-1/2} e^{-E_0/RT}. \quad (12)$$

This equation relates to the classical Arrhenius relationship and differs only in the temperature-dependent pre-exponential factor, $T^{n-1/2}$, and in the entrance barrier, E_0 , vs. the activation energy E_a . The experimentally available A coefficients (Table 3), can be utilized to calculate the constant C .

Due to the uniqueness of the Laplacian formalism we can extract energy dependent cross sections for suprathermal reactants from given thermal reaction rates. Since $n = 1/2$ for all reactions of interest (Table 3) we can correlate the thermal rate constant $k(T)$ data via Eq. (12) with the cross section $\sigma(E)$, Eq. (9), to

$$k(T) = Ae^{-E_0/RT} \Leftrightarrow \sigma(E) = C \frac{(E - E_0)^{1/2}}{E}. \quad (13)$$

It is important to note that the correlation between the rate constant $k(T)$ and the cross section $\sigma(E)$ in Eq. (13) must be modified using the experimental activation energy E_a . Classically, the latter is defined as the slope of the logarithmic plot of $k(T)$ vs. $1/T$. Heyl and Roessler (1990) calculated the correlation between the experimentally determined activation energy E_a and the entrance barrier E_0 to

$$E_a \approx E_0 + \left(n - \frac{1}{2}\right) RT. \quad (14)$$

Since for all of the relevant reactions, $n = 1/2$ (cf. Table 3), the values of E_0 and E_a are identical. Now we are able to derive an expression for the suprathermal rate constant $k(E)$. The energy-dependent cross section $\sigma(E)$ relates to $k(E)$ via Eq. (15). This relationship also works because the kinetic energy of a hydride is small in comparison to the kinetic energy of a suprathermal hydrogen atom:

$$k(E) = \sigma(E)|\vec{v}_r| = \sigma(E)\sqrt{\frac{2E}{\mu}}. \quad (15)$$

Plugging Eq. (9) into Eq. (15) gives

$$\begin{aligned} k(E) &= C \frac{(E - E_0)^{1/2}}{E} \sqrt{\frac{2E}{\mu}} \\ &= \frac{A(\pi\mu)^{1/2}(E - E_0)^{1/2}}{2^{3/2}\Gamma(3/2)E} \sqrt{\frac{2E}{\mu}}. \end{aligned} \quad (16)$$

Eq. (16) relates $k(E)$ to A and E , allowing both to be calculated using the available thermal data (cf. Table 3).

3. Results and discussion

3.1. Thermal rate constants

Table 6 compiles the thermal rate constants for the reaction of the saturated hydrides with atomic hydrogen (Table 3) calculated for characteristic temperatures of the atmospheres of outer solar system planets and their moons (Table 2).

As evident the calculated thermal rate constants vary significantly from 3.31×10^{-12} to $8.26 \times 10^{-73} \text{ cm}^3 \text{ s}^{-1}$. These very low rate constants are based on the inherent low-temperatures of the planetary atmospheres and the incapability of the reactants to overcome the activation energy. Since fast reactions are classified by a rate constant of about $10^{-10} \text{ cm}^3 \text{ s}^{-1}$ (cf. Section 1), the reaction of thermal hydrogen with saturated hydrides are expected to be

Table 6
The rate constants $k(T)$ for various reactions of simple saturated hydrides ($\text{cm}^3 \text{s}^{-1}$)

Hydride	Jupiter	Saturn	Uranus	Neptune
CH ₄	5.42×10^{-26}	1.59×10^{-29}	7.19×10^{-44}	5.90×10^{-46}
GeH ₄	2.06×10^{-13}	4.22×10^{-14}	6.80×10^{-17}	2.70×10^{-17}
NH ₃	5.59×10^{-26}	1.83×10^{-29}	1.30×10^{-43}	1.17×10^{-45}
PH ₃	5.11×10^{-13}	1.81×10^{-13}	2.69×10^{-15}	1.46×10^{-15}
AsH ₃	3.31×10^{-12}	1.21×10^{-12}	—	—
H ₂ O	1.57×10^{-37}	9.03×10^{-44}	4.01×10^{-69}	8.26×10^{-73}
H ₂ S	8.69×10^{-14}	2.60×10^{-14}	2.10×10^{-16}	1.00×10^{-16}

Only CH₄ has been detected on Pluto, Titan, and Triton. The rate constants are 5.65×10^{-68} , 1.60×10^{-37} , and $3.06 \times 10^{-37} \text{ cm}^3 \text{ s}^{-1}$, respectively. The temperature for Pluto has been taken as 44 K.

Table 7
Reduced mass and constant C for reactions of atomic hydrogen with various hydrides

Reaction	Reduced mass, μ (kg mol^{-1})	Constant, C ($\text{kg}^{1/2} \text{ cm}^3 \text{ mol}^{-1/2} \text{ s}^{-1}$)
CH ₄ + H	9.48×10^{-4}	2.18×10^{-12}
SiH ₄ + H	9.77×10^{-4}	5.08×10^{-13}
GeH ₄ + H	9.95×10^{-4}	4.33×10^{-12}
NH ₃ + H	9.52×10^{-4}	2.64×10^{-12}
PH ₃ + H	9.79×10^{-4}	9.96×10^{-12}
AsH ₃ + H	9.95×10^{-4}	5.73×10^{-12}
H ₂ O + H	9.55×10^{-4}	3.28×10^{-12}
H ₂ S + H	9.79×10^{-4}	3.32×10^{-12}

very slow. However, the reactions of PH₃ and AsH₃ with atomic hydrogen on Jupiter and Saturn have reaction rates of 10^{-12} – $10^{-13} \text{ cm}^3 \text{ s}^{-1}$. Therefore these reactions might be relevant even in these low-temperature environments. In the following paragraph, these thermal rate constants will be compared with their suprathermal counterparts to determine the relevance of these reactions in the atmosphere of the outer solar system planets and their moons.

3.2. Suprathermal rate constants

The suprathermal rate constants $k(E)$ have been calculated using Eq. (16) using reduced masses and constants C as compiled in Table 7. Table 8 compiles suprathermal rate

constants at selected kinetic energies of the hydrogen atoms. These data range from 2×10^{-11} to $4 \times 10^{-10} \text{ cm}^3 \text{ s}^{-1}$. Compared to the thermal rate constants, this is at least two orders of magnitude larger than the maximum thermal rate constants calculated of the H/AsH₃ system (Table 6). These data alone imply a significant increase in the reactivity of suprathermal hydrogen atoms compared to thermal ones. Plots of thermal and suprathermal rate constants versus the temperature and kinetic energy of the hydrogen atom, respectively, were also prepared (Figs. 1–8). This gives a quantitative and graphical comparison of how the two rate constants $k(E)$ and $k(T)$ vary with a change in kinetic energy and temperature.

These graphs show common features for all systems investigated. The plots of the suprathermal rate constants $k(E)$ start at a well-defined threshold energy, the entrance barrier E_0 . Below E_0 , the rate constant $k(E)$ is zero. As the kinetic energy of the suprathermal H atom rises, the $k(E)$ graphs increase steeply reaching a plateau in the region of 0.5–1.0 eV. The curves of the thermal rate constant $k(T)$ versus the temperature form an elongated s-shaped graph each with two points of inflection; these graphs intersect the $k(E)$ plots before reaching the plateau. For each system, even at very low-temperatures $k(T)$ has a finite value. As the temperature increases, the $k(T)$ versus T graphs also reach plateaus; but the underlying rate constants are always lower than the corresponding suprathermal rate constants $k(E)$.

Table 8
Rate constant $k(E)$ of suprathermal hydrogen atoms with various saturated hydrides at selected collision energies

Hydride	0.5 eV	1.0 eV	1.5 eV	2.0 eV
CH ₄	n.r.	7.08×10^{-11}	8.18×10^{-11}	8.67×10^{-11}
SiH ₄	2.00×10^{-11}	2.16×10^{-11}	2.20×10^{-11}	2.23×10^{-11}
GeH ₄	1.74×10^{-10}	1.84×10^{-10}	1.88×10^{-10}	1.89×10^{-10}
NH ₃	n.r.	7.22×10^{-11}	8.84×10^{-11}	9.55×10^{-11}
PH ₃	4.22×10^{-10}	4.36×10^{-10}	4.41×10^{-10}	4.43×10^{-10}
AsH ₃	2.41×10^{-10}	2.49×10^{-10}	2.52×10^{-10}	2.53×10^{-10}
H ₂ O	n.r.	5.20×10^{-11}	9.65×10^{-11}	1.12×10^{-10}
H ₂ S	1.39×10^{-10}	1.45×10^{-10}	1.47×10^{-10}	1.47×10^{-10}

n.r. = no reaction.

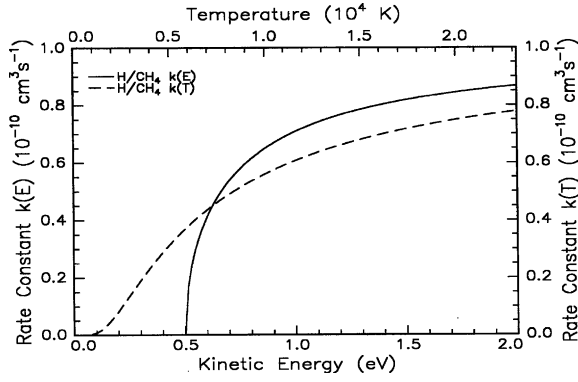


Fig. 1. Energy and temperature dependence of the suprathermal rate constant $k(E)$ and the thermal rate constant $k(T)$ for the H/CH₄ system.

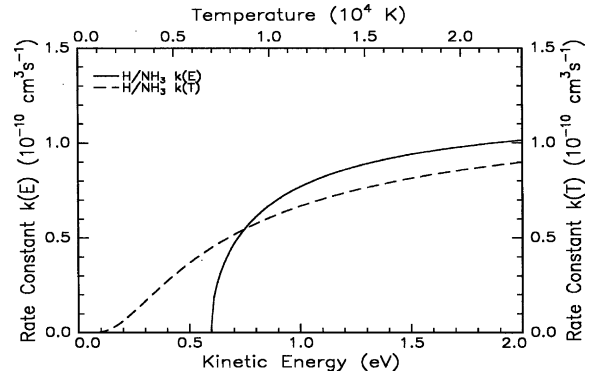


Fig. 4. Energy and temperature dependence of the suprathermal rate constant $k(E)$ and the thermal rate constant $k(T)$ for the H/NH₃ system.

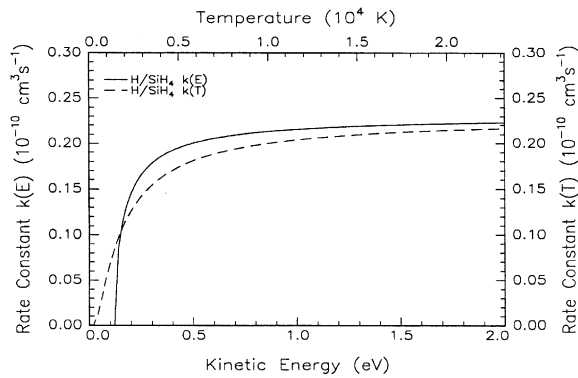


Fig. 2. Energy and temperature dependence of the suprathermal rate constant $k(E)$ and the thermal rate constant $k(T)$ for the H/SiH₄ system.

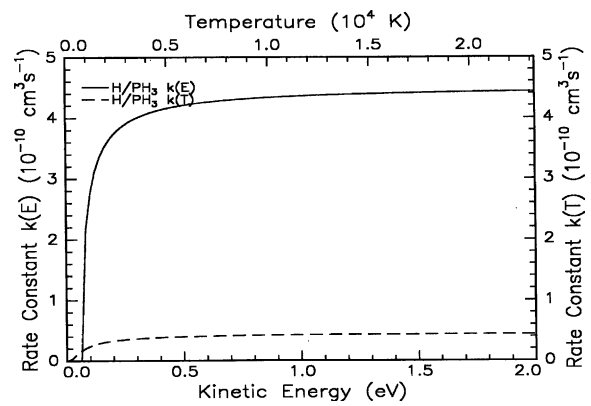


Fig. 5. Energy and temperature dependence of the suprathermal rate constant $k(E)$ and the thermal rate constant $k(T)$ for the H/PH₃ system.

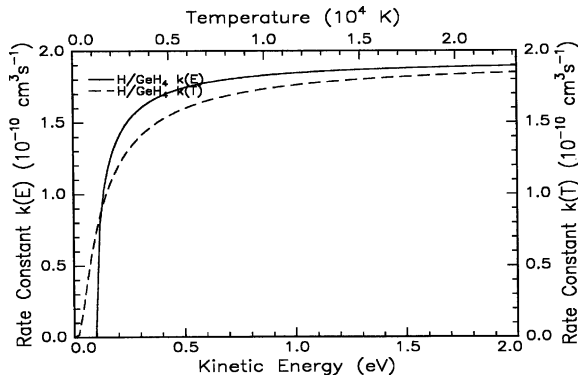


Fig. 3. Energy and temperature dependence of the suprathermal rate constant $k(E)$ and the thermal rate constant $k(T)$ for the H/GeH₄ system.

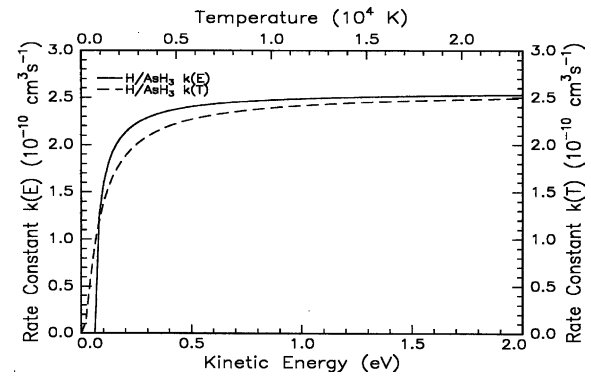


Fig. 6. Energy and temperature dependence of the suprathermal rate constant $k(E)$ and the thermal rate constant $k(T)$ for the H/AsH₃ system.

4. Conclusions

In this paper, we investigated the kinetics of various saturated hydrides reacting with thermal and suprathermal hydrogen atoms in the low-temperature atmospheres of Jupiter, Saturn, Uranus, Neptune, Pluto, Titan, and Triton. Our data reveal that all suprathermal rate constants are temperature independent and as large as $10^{-10} \text{ cm}^3 \text{ s}^{-1}$. Thermal coun-

terparts were found to be—in particular at the prevailing low atmospheric temperatures—as low as $10^{-73} \text{ cm}^3 \text{ s}^{-1}$. These data alone suggest a significantly enhanced reactivity of suprathermal hydrogen atoms in atmospheres of planets and their satellites. Therefore, future atmospheric models simulating the chemical evolution of outer solar system planets and their moons should include this

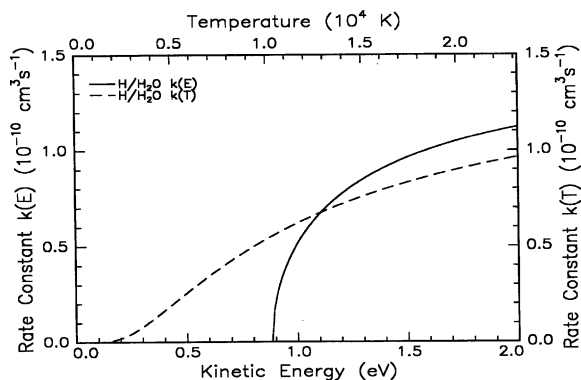


Fig. 7. Energy and temperature dependence of the suprathreshold rate constant $k(E)$ and the thermal rate constant $k(T)$ for the $\text{H}/\text{H}_2\text{O}$ system.

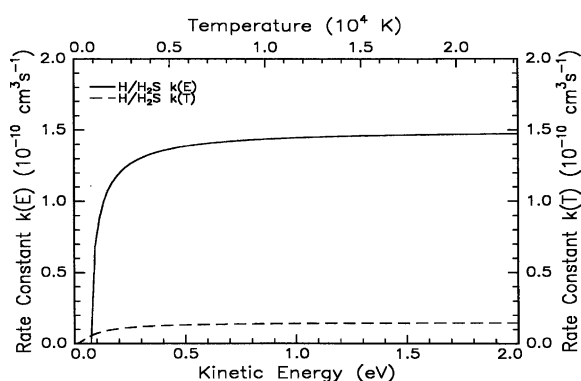


Fig. 8. Energy and temperature dependence of the suprathreshold rate constant $k(E)$ and the thermal rate constant $k(T)$ for the $\text{H}/\text{H}_2\text{S}$ system.

reaction class. Since suprathreshold hydrogen atoms are strongly expected to be generated via photolyses of saturated hydrides themselves or organic molecules, photochemical models need also wavelength-dependent photodissociation cross section and the translational energy distribution of the suprathreshold hydrogen atoms. The actual effect on the planetary chemistry depends also on the branching ratio of reactive collisions versus the gravitational escape of the suprathreshold hydrogen atoms. These consideration makes it clear that an inclusion of suprathreshold pathways into currently existing models is not trivial—but a challenging task for the future.

Acknowledgements

This work has been supported by The University of York United Kingdom. It has been carried out within the International Astrophysics Network (<http://www.chem.hawaii.edu/Bil301/network.htm>).

References

Arfken, G., 1985. *Mathematical Methods for Physicists*. Academic Press, Inc., Harcourt Brace Jovanovich, Publishers, Boston.

- Atkins, P.W., 1999. *Physical Chemistry*. Oxford University Press, Oxford.
- Baines, K.H., Hammel, H.B., 1994. Clouds, hazes, and the stratospheric methane abundance in Neptune. *Icarus* 109, 20–39.
- Baines, K.H., Mickelson, M.E., Larson, L.E., Ferguson, D.W., 1995. The abundances of methane and ortho/para hydrogen on Uranus and Neptune—implications of new laboratory 4-0 H-2 quadrupole line parameters. *Icarus* 114, 328–340.
- Balucani, N., Asvany, O., Osamura, Y., Huang, L.C.L., Lee, Y.T., Kaiser, R.I., 2000. Laboratory investigation on the formation of unsaturated nitriles in Titans atmosphere. *Planet. Space Sci.* 48, 447–462.
- Bergin, E.A., Lellouch, E., Harwit, M., Gurwell, M.A., et al., 2000. Submillimeter wave astronomy satellite observations of Jupiter and Saturn: detection of 557 GHz water emission from the upper atmosphere. *Astrophys. J.* 539, 1147–1150.
- Borunov, S., Dorofeeva, V., Khodakovskiy, I., Drossart, P., et al., 1995. Phosphorus chemistry in the atmosphere of Jupiter—a reassessment. *Icarus* 113, 460–464.
- Borysow, A., Tang, C.M., 1993. Far infrared CIA spectra of $\text{N}_2\text{-CH}_4$ pairs for modeling of Titans atmosphere. *Icarus* 105, 175–183.
- Chen, F.Z., Judge, D.L., Wu, C.Y.R., Caldwell, J., et al., 1991. High-resolution, low-temperature photoabsorption cross sections of C_2H_2 , PH_3 , AsH_3 , and GeH_4 , with application to Saturn's atmosphere. *J. Geophys. Res. Planets* 96, 17519–17527.
- Davis, G.R., Naylor, D.A., Griffin, M.J., Clark, T.A., et al., 1997. Broadband submillimeter spectroscopy of HCN , NH_3 , and PH_3 , in the troposphere of Jupiter. *Icarus* 130, 387–403.
- Debergh, C., Lutz, B.L., Owen, T., Maillard, J.P., 1990. Monodeuterated methane in the outer solar system. 4. its detection and abundance on Neptune. *Astrophys. J.* 355, 661–666.
- Deboer, D.R., Steffes, P.G., 1994. Laboratory measurements of the microwave properties of H_2S under simulated Jovian conditions with an application to Neptune. *Icarus* 109, 352–366.
- Degraauw, T., Feuchtgruber, H., Bezaud, B., Drossart, P., et al., 1997. First results of ISO-SWS observations of Saturn: detection of CO_2 , $\text{CH}_3\text{C}_2\text{H}$, C_4H_2 and tropospheric H_2O . *Astron. Astrophys.* 321, 113–116.
- Delgenio, A.D., McGrattan, K.B., 1990. Moist convection and the vertical structure and water abundance of Jupiter's atmosphere. *Icarus* 84, 29–53.
- de Pater, I., Romani, P.N., Atreya, S.K., 1991. Possible microwave absorption by H_2S gas in Uranus and Neptune's atmospheres. *Icarus* 91, 220–233.
- de Pater, I., Dunn, D., Romani, P., Zahnle, K., 2001. Reconciling Galileo probe data and groundbased radio observations of ammonia on Jupiter. *Icarus* 149, 66–78.
- Dowling, T.E., Ingersoll, A.P., 1989. Jupiter's great red spot as a shallow water system. *J. Atmos. Sci.* 46, 3256–3278.
- Edgington, S.G., Atreya, S.K., Trafton, L.M., Caldwell, J.J., et al., 1998. On the latitude variation of ammonia, acetylene, and phosphine altitude profiles on Jupiter from HST Faint Object Spectrograph observations. *Icarus* 133, 192–209.
- Edgington, S.G., Atreya, S.K., Trafton, L.M., Caldwell, J.J., et al., 1999. Ammonia and eddy mixing variations in the upper troposphere of Jupiter from HST Faint Object Spectrograph observations. *Icarus* 142, 342–356.
- Encenaz, T., Schulz, R., Stuwe, J.A., Wiedemann, G., et al., 1995. Near-IR spectroscopy of Jupiter at the time of comet Shoemaker-Levy 9 impacts—emissions of CH_4 , H-3(+) and H-2(+) . *Geophys. Res. Lett.* 22, 1577–1580.
- Encenaz, T., Serabyn, E., Weisstein, E.W., 1996. Millimeter spectroscopy of Uranus and Neptune: constraints on CO and PH_3 tropospheric abundances. *Icarus* 124, 616–624.
- Ferris, J.P., Jacobson, R.R., Guillemin, J.C., 1992. The photolysis of NH_3 in the presence of substituted acetylenes—a possible source of oligomers and HCN on Jupiter. *Icarus* 95, 54–59.

- Folkner, W.M., Woo, R., Nandi, S., 1998. Ammonia abundance in Jupiter's atmosphere derived from the attenuation of the Galileo probe's radio signal. *J. Geophys. Res. Planets* 25, 22847–22855.
- Fouchet, T., Lellouch, E., Bezdard, B., Encrenaz, T., et al., 2000. ISO-SWS observations of Jupiter: measurement of the ammonia tropospheric profile and of the N-15/N-14 isotopic ratio. *Icarus* 143, 223–243.
- Gibbard, S., Levy, E.H., Lunine, J.I., 1995. Generation of lightning in Jupiter's water cloud. *Nature* 378, 592–595.
- Griffith, C.A., Bezdard, B., Owen, T., Gautier, D., 1992. The tropospheric abundances of NH₃ and PH₃ in Jupiter's great red spot, from Voyager iris observations. *Icarus* 98, 82–93.
- Herbert, F., Sandel, B.R., 1991. CH₄ and haze in Triton's lower atmosphere. *J. Geophys. Res. Planets* 96, 19241–19252.
- Heyl, M., 1990. Chemische Reaktionen suprathermischer Wasserstoffatome in der Koma von Kometen. *Forschungszentrum Jülich, Berichte Nr. 2409*.
- Heyl, M., Roessler, K., 1990. *Handbook of Hot Atom Chemistry*. VCH Publishers, Cambridge.
- Hofstadter, M.D., Muhleman, D.O., 1989. Latitudinal variations of ammonia in the atmosphere of Uranus—an analysis of microwave observations. *Icarus* 81, 396–412.
- Joiner, J., Steffes, P.G., Noll, K.S., 1992. Search for sulfur (H₂S) on Jupiter at millimeter wavelengths. *IEEE Trans. Microwave Theory Tech.* 40, 1101–1109.
- Kaiser, R.I., 2002. An experimental investigation on the formation of carbon-bearing molecules in the interstellar medium via neutral–neutral reactions. *Chem. Rev.* 102, 1309–1358.
- Karkoschka, E., 1994. Spectrophotometry of the Jovian planets and Titan at 300 nm to 1000 nm wavelength—the methane spectrum. *Icarus* 111, 174–192.
- Karkoschka, E., 1998. Methane, ammonia, and temperature measurements of the Jovian planets and Titan from CCD-spectrophotometry. *Icarus* 133, 134–146.
- Kim, S.J., Geballe, T.R., Noll, K.S., 2000. Three-micrometer CH₄ line emission from Titan's high-altitude atmosphere. *Icarus* 147, 588–591.
- Lara, L.M., Bezdard, B., Griffith, C.A., Lacy, J.H., et al., 1998. High-resolution 10-micrometer spectroscopy of ammonia and phosphine lines on Jupiter. *Icarus* 131, 317–333.
- Lide, D.R., 1999. *Handbook of Chemistry and Physics*. CRC Press, Boca Raton.
- Lunine, J.I., Yung, Y.L., Lorenz, R.D., 1999. On the volatile inventory of Titan from isotopic abundances in nitrogen and methane. *Planet. Space Sci.* 47, 1291–1303.
- Maillard, J.P., Drossart, P., Bezdard, B., Debergh, C., et al., 1995. Methane and carbon monoxide infrared emissions observed at the Canada-France-Hawaii telescope during the collision of comet SL-9 with Jupiter. *Geophys. Res. Lett.* 22, 1573–1576.
- Mallard, W.G., 1994. *NIST Chemical Kinetics*. National Institute of Standards and Technology, Gaithersburg.
- McKay, C.P., Martin, S.C., Griffith, C.A., Keller, R.M., 1997. Temperature lapse rate and methane in Titan's troposphere. *Icarus* 129, 498–505.
- Molina, A., Moreno, F., 1992. Equivalent widths of the CH₄ 6190 and NH₃ 6450 bands across Jupiter's disk—variations from 1985 to 1989. *Astron. Astrophys.* 256, 299–304.
- Moreno, F., Molina, A., Lara, L.M., 1991. Charge-coupled device spectral images of spatially resolved regions of Jupiter in the 6190 and 8900 methane and 6450 ammonia bands during the 1989 opposition. *J. Geophys. Res. Space Phys.* 96, 14119–14127.
- Nava, D.F., Payne, W.A., Marston, G., Stief, L.J., 1993. The reaction of atomic hydrogen with germane temperature dependence of the rate constant and implications for germane photochemistry in the atmospheres of Jupiter and Saturn. *J. Geophys. Res. Planets* 98, 5531–5537.
- Noll, K.S., Larson, H.P., 1991. The spectrum of Saturn from 1990 to 2230 cm⁻¹—abundances of AsH₃, CH₃D, CO, GeH₄, NH₃, and PH₃. *Icarus* 89, 168–189.
- Noll, K.S., Geballe, T.R., Knacke, R.F., 1995. Detection of (H₂O)-O-18 in Jupiter. *Astrophys. J.* 453, 149–153.
- Ollivier, J.L., Dobrijevic, M., Parisot, J.P., 2000. New photochemical model of Saturn's atmosphere. *Planet. Space Sci.* 48, 699–716.
- Ortiz, J.L., Moreno, F., Molina, A., 1992. Spectroscopic observations at different regions of Jupiter during the 1991 opposition—absolute reflectivities and CH₄ 6190 and NH₃ 6450 absorption bands. *Astron. Astrophys.* 260, 465–472.
- Ortiz, J.L., Moreno, F., Molina, A., 1993. Absolutely calibrated CCD images of Saturn at methane band and continuum wavelengths during its 1991 opposition. *J. Geophys. Res. Planets* 98, 3053–3063.
- Orton, G.S., Serabyn, E., Lee, Y.T., 2000. Vertical distribution of PH₃ in Saturn from observations of its 1-0 and 3-2 rotational lines. *Icarus* 146, 48–59.
- Ricard, A., Cernogora, G., Fitaire, M., Hochard, L., et al., 1995. Measurements in N-2-CH₄(C₂H₂) discharges of reaction rates and thermochemical constants for Titan atmosphere study. *Planet. Space Sci.* 43, 41–46.
- Rodgers, S.D., Charnley, S.B., 1998. HNC and HCN in comets. *Astrophys. J.* 501, L227–230.
- Romani, P.N., Atreya, S.K., 1989. Stratospheric aerosols from CH₄ photochemistry on Neptune. *Geophys. Res. Lett.* 16, 941–944.
- Romani, P.N., Bishop, J., Bezdard, B., Atreya, S., 1993. Methane photochemistry on Neptune—ethane and acetylene mixing ratios and haze production. *Icarus* 106, 442–463.
- Roos-Serote, M., Drossart, P., Encrenaz, T., Lellouch, E., et al., 1998. Analysis of Jupiter north equatorial belt hot spots in the 4–5 μm range from Galileo near-infrared mapping spectrometer observations: measurements of cloud opacity, water, and ammonia. *J. Geophys. Res. Planets* 25, 23023–23041.
- Sada, P.V., Bjoraker, G.L., Jennings, D.E., McCabe, G.H., et al., 1998. Observations of CH₄, C₂H₆, and C₂H₂ in the stratosphere of Jupiter. *Icarus* 136, 192–201.
- Samuelson, R.E., Mayo, L.A., 1997. Steady-state model for methane condensation in Titan's troposphere. *Planet. Space Sci.* 45, 949–958.
- Samuelson, R.E., Nath, N.R., Borysow, A., 1997. Gaseous abundances and methane supersaturation in Titan's troposphere. *Planet. Space Sci.* 45, 959–980.
- Satoh, T., Kawabata, K., 1992. Methane band photometry of the faded south equatorial belt of Jupiter. *Astrophys. J.* 384, 298–304.
- Simon-Miller, A.A., Conrath, B., Gierasch, P.J., Beebe, R.F., 2000. A detection of water ice on Jupiter with Voyager iris. *Icarus* 145, 454–461.
- Smith, I.W.M., Rowe, B.R., 2000. Reactions at very low-temperatures: laboratory of interstellar chemistry. *Acc. Chem. Res.* 33, 261–268.
- Smith, W.H., Conner, C.P., Baines, K.H., 1990. Absorption coefficients for the 6190 CH₄ band between 290 K and 100 K with application to Uranus atmosphere. *Icarus* 85, 58–64.
- Stansberry, J.A., Spencer, J.R., Schmitt, B., Benchkoura, A.I., et al., 1996. A model for the overabundance of methane in the atmospheres of Pluto and Triton. *Planet. Space Sci.* 44, 1051–1063.
- Strobel, D.F., Summers, M.E., Herbert, F., Sandel, B.R., 1990. The photochemistry of methane in the atmosphere of Triton. *Geophys. Res. Lett.* 17, 1729–1732.
- Strong, K., Taylor, F.W., Calcutt, S.B., Remedios, J.J., et al., 1993. Spectral parameters of self-broadened and hydrogen-broadened methane from 2000 cm⁻¹ to 9500 cm⁻¹ for remote sounding of the atmosphere of Jupiter. *J. Quant. Spectrosc. Radiat. Transfer* 50, 363–429.
- Thompson, W.R., Henry, T.J., Schwartz, J.M., Khare, B.N., et al., 1991. Plasma discharge in N₂—experimental results and applications to Titan. (CH₄ at low pressures). *Icarus* 90, 57–73.
- Thompson, W.R., Zollweg, J.A., Gabis, D.H., 1992. Vapor–liquid equilibrium thermodynamics of N₂—model and Titan applications (CH₄). *Icarus* 97, 187–199.

- Tokano, T., Neubauer, F.M., Laube, M., McKay, C.P., 2001. Three-dimensional modeling of the tropospheric methane cycle on Titan. *Icarus* 153, 130–147.
- Weisstein, E.W., Serabyn, E., 1994. Detection of the 267 GHz $J = 1-0$ rotational transition of PH_3 in Saturn with a new Fourier transform spectrometer. *Icarus* 109, 367–381.
- Wilson, E.H., Atreya, S.K., 2000. Sensitivity studies of methane photolysis and its impact on hydrocarbon chemistry in the atmosphere of Titan. *J. Geophys. Research-Planets* 105, 20263–20273.
- Yung, Y.L., DeMore, W.B., 1999. *Photochemistry of Planetary Atmospheres*. Oxford University Press, Oxford.